Journal of Power Sources 194 (2009) 88–92

Contents lists available at ScienceDirect

Journal of Power Sources

journal homepage: www.elsevier.com/locate/jpowsour

Short communication

Structural and transport properties of $Li_xNi_{1-y-z}Co_yMn_zO_2$ cathode materials

J. Molenda*, A. Milewska

Department of Solid State Chemistry, Faculty of Materials Science and Ceramics, AGH University of Science and Technology, al. Mickiewicza 30, 30-059 Kraków, Poland

ARTICLE INFO

Article history:
Received 17 October 2008
Received in revised form 8 December 2008
Accepted 9 December 2008
Available online 24 December 2008

Keywords:
Li-ion batteries
Cathode material
$Li_xNi_{1-y-z}Co_yMn_zO_2$
Intercalation
Transport properties

ABSTRACT

In this work structural and transport properties of layered $LiNi_{1-y-z}Co_yMn_zO_2$ ($y = 0.25$, 0.35, 0.5 and $z = 0.1$) cathode materials are presented. In the considered group of oxides, $LiNi_{1-y-z}Co_yMn_zO_2$, there is no clear correlation between electrical conductivity and the *a* parameter (M–M distance in the octahedra layers). A non-monotonic modification of electrical properties of $Li_xNi_{0.65}Co_{0.25}Mn_{0.1}O_2$ cathode materials is observed upon lithium deintercalation.

© 2009 Elsevier B.V. All rights reserved.

1. Introduction

Searching for an optimal composition of a cathode material for Li-ion reversible cells leads to layered 3d transition metal oxides having Li_xMO_2 formula, in which lithium intercalation proceeds via topotactic, redox type reaction, ensuring high effectiveness of the intercalation process. The reduction of the transition metal ions $M^{4+} \rightarrow M^{3+} \rightarrow M^{2+}$ progressing in the course of the intercalation process leads to the change of their ionic radii within the 0.5–0.8 Å range, but fortunately it does not destroy the crystal structure. Moreover, the 3d oxides exhibit supreme potentials versus lithium anode, when compared to other transition metal compounds (4d oxides, sulphides, selenides) and the cathode potential increases with the number of 3d electrons [1]. It seems that there is still vast potential for improving electrochemical properties of layered $LiCoO_2$ and $LiNiO_2$-based cathode materials. Mainly, in terms of their chemical stability and, as a consequence, reversible capacity.

$LiNi_{1-y-z}Co_yMn_zO_2$ type complex oxides are relatively new cathode materials which properties are currently under intensive investigations. Electrochemical properties of these materials can be strongly modified by their composition and are not easy to predict. The main goal of this paper was to obtain material with good transport properties and good chemical stability, which in turn may lead to an improved reversible capacity of the cell.

2. Experimental

$LiNi_{1-y-z}Co_yMn_zO_2$ materials were synthesized by a soft chemistry EDTA-based method, which detailed description is given elsewhere [2]. Li_2CO_3 (POCh, p.p.a.), $C_4H_6MnO_4{\cdot}4H_2O$ (Fluka, p.p.a.), $Co(NO_3)_2{\cdot}6H_2O$ (POCh, p.p.a.) and $Ni(NO_3)_2{\cdot}6H_2O$ (Aldrich, p.p.a.) were put in a minimal amount of deionized water. While stirring the solution, $C_6H_8O_7{\cdot}H_2O$ was added to dissolve Li_2CO_3. Then, ammonia salt of EDTA was added to the mixture as a complexing agent. The obtained solutions were heated in evaporating quartz dishes, the temperature was gradually raised from 100 to 400 °C. A precursor xerogels were thoroughly mixed in mortar, formed into pellets and heated at 800 °C in air for 1 h. This step was introduced in order to minimize the amount of residual carbon after EDTA and citric acid decomposition. After cooling to room temperature the samples were grounded in mortar, pressed uniaxially (100 MPa) into pellets. The pellets were finally sintered at 950 °C for 18 h in air and then quenched to room temperature. Obtained samples were stored in exsiccator containing P_2O_5 powder.

The crystal structure of the samples was characterized by X-ray diffraction (XRD) method using an X-ray diffractometer (Philips X'Pert Pro) with Cu Kα radiation. The X-ray patterns were analyzed using Rietveld method with GSAS/EXPGUI software [3,4].

To examine transport properties of the deintercalated samples, lithium cells assembled from $LiNi_{0.65}Co_{0.25}Mn_{0.1}O_2$ cathode materials, metallic lithium anode and 1 M $LiPF_6$ in ethylene carbonate (EC)/dimethyl carbonate (DMC) electrolyte were constructed in argon filled glove-box. Deintercalation process was performed under a constant current of 100 μA cm^{-2} until intended x_{Li} val-

* Corresponding author. Tel.: +48 12 6172522; fax: +48 12 6172522.
E-mail addresses: molenda@agh.edu (J. Molenda), annamilew@wp.pl (A. Milewska).

0378-7753/$ – see front matter © 2009 Elsevier B.V. All rights reserved.
doi:10.1016/j.jpowsour.2008.12.033

ues were obtained. The process was performed using computer controlled amperostat Kest 32k.

Before electrical measurements the samples were rinsed in hexane from electrolyte residuals, pumped out in glass tube and then grinded on abrasive paper. Electrical conductivity was measured using a four-electrode alternating-current method. Thermoelectric power was measured dynamically, by measuring the potential difference and temperature difference (ΔT up to 2°) at the ends of the sample. The measurements in the temperature range of 200–350 K were carried out under vacuum ($\sim 10^{-2}$ mbar).

3. Results and discussion

3.1. Structural properties of pristine $LiNi_{1-y-z}Co_yMn_zO_2$ oxides

Our previous works performed for the series of $LiNi_{1-y}Co_yO_2$ cathode oxides [5,6] showed that $LiNi_{0.75}Co_{0.25}O_2$ composition demonstrates the best transport and electrochemical properties. In this work we use this material as the reference one. It will be shown how further substitution of nickel with cobalt and manganese influences the structural and transport properties of complex $LiNi_{1-y-z}Co_yMn_zO_2$ oxides. Fig. 1 shows X-ray diffraction patterns of the starting $LiNi_{1-y-z}Co_yMn_zO_2$ cathode materials. All synthesized compounds have a layered structure and all peaks can be indexed on the basis of the α-$NaFeO_2$ structure (space group *R*-3*m*, trigonal), in which the transition metal ions are surrounded by six oxygen atoms. Layers of $((Ni,Co,Mn)O_2)_n$ are formed out from edge-sharing $(Ni,Co,Mn)O_6$ octahedras with intercalating lithium ions located between the layers. The layered structure of the analyzed materials and homogenous distribution of cations are shown by the splitting of the (0 1 8)/(1 1 0) peaks and the intensity ratio of the (0 0 3) and (1 0 4) peaks [7]. The values of *a* and *c* parameters estimated on the basis of Rietveld analysis are presented in Table 1. This data indicate that substitution of nickel with manganese raises the structural parameters *a* and *c* significantly, while further substitution of nickel with cobalt shrinks the lattice along both *a* and *c* axes. High (0 0 3)/(1 0 4) peaks ratio is related to the low values of *z* parameter (which reflects Li^+ and Ni^{2+} cation disorder). One can notice that an increase of cobalt amount suppress the occurrence of the cation mixing (Table 1).

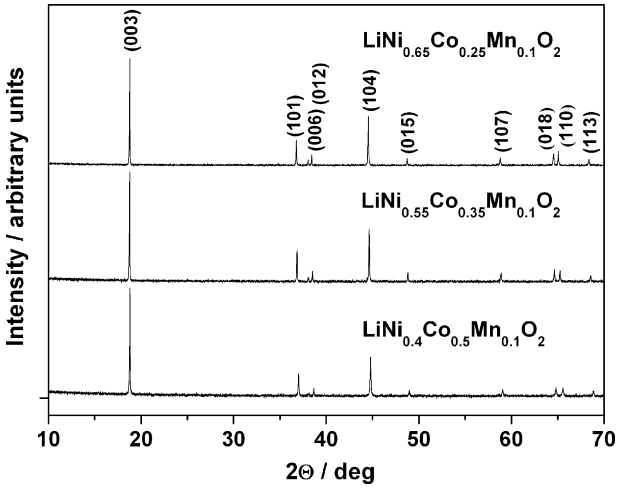

Fig. 1. X-ray diffraction patterns for $LiNi_{1-y-z}Co_yMn_zO_2$ oxides obtained by a soft chemistry EDTA method (calcinated at 950 °C).

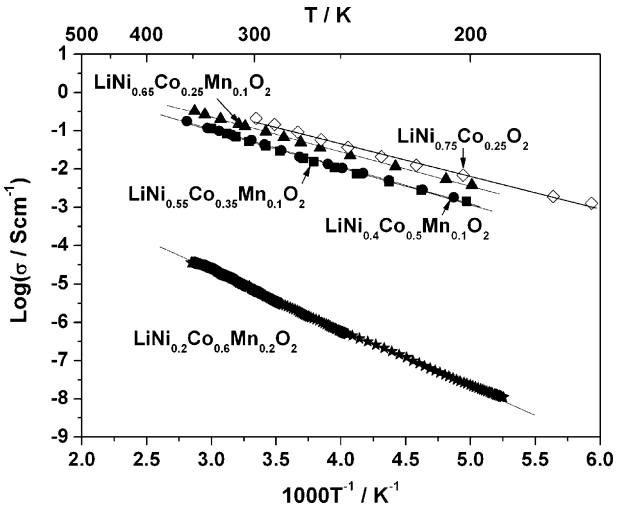

Fig. 2. Temperature dependence of electrical conductivity for the $LiNi_{1-y-z}Co_yMn_zO_2$ and $LiNi_{0.75}Co_{0.25}O_2$ oxides.

3.2. Electronic conductivity and thermoelectric power of pristine $LiNi_{1-y-z}Co_yMn_zO_2$ oxides

Fig. 2 shows the temperature dependence of the electrical conductivity for $LiNi_{1-y-z}Co_yMn_zO_2$ oxides. The conductivities of $LiNi_{1-y-z}Co_yMn_zO_2$ oxides are compared with the conductivity of $LiNi_{0.75}Co_{0.25}O_2$ reference oxide. Substitution of 0.1 mol of Ni with Mn ions in $LiNi_{0.75}Co_{0.25}O_2$ oxide slightly decreases electrical conductivity and changes the activation energy of conductivity from 0.16 eV for $LiNi_{0.75}Co_{0.25}O_2$ to 0.18 eV for $LiNi_{0.65}Co_{0.25}Mn_{0.1}O_2$ (Fig. 2, Table 2). When the amount of Mn increases to 0.2 mol in $LiNi_{0.2}Co_{0.6}Mn_{0.2}O_2$ the conductivity drops few orders of magnitude and exhibits high activation energy, 0.3 eV (Fig. 2, Table 2). Strong deterioration of the electrical conductivity of $LiNi_{0.5-y}Co_{2y}Mn_{0.5-y}O_2$ oxides containing high amount of manganese has been also noticed by Choi and Manthiram [8]. It seems that in the considered group of oxides there is no clear correlation between electrical conductivity and the *a* parameter (M–M distance in the octahedra layers, Table 1), observed often for simple layered transition metal oxides [6,9,10].

The temperature dependence of the thermoelectric power (α) for the $LiNi_{1-y-z}Co_yMn_zO_2$ and $LiNi_{0.75}Co_{0.25}O_2$ oxides is shown in Fig. 3. The sign of the thermoelectric power is positive indicating that electronic holes are predominant in charge transport, however the character of the temperature dependence of α of $LiNi_{1-y-z}Co_yMn_zO_2$ oxides indicates that the transport occurs in more than one band. Higher number of charge carriers in $LiNi_{0.75}Co_{0.25}O_2$ reference oxide corresponds with lower value of the thermoelectric power and lower value of the activation energy

Table 1
Structural parameters for $LiNi_{1-y-z}Co_yMn_zO_2$ oxides.

Composition	*a* parameter/Å	*c* parameter/Å	*z* parameter/at.%
$LiNi_{0.75}Co_{0.25}O_2$	2.860(1)	14.150(2)	
$LiNi_{0.65}Co_{0.25}Mn_{0.1}O_2$	2.8663(3)	14.196(3)	2.7
$LiNi_{0.55}Co_{0.35}Mn_{0.1}O_2$	2.8576(3)	14.179(3)	0.5
$LiNi_{0.4}Co_{0.5}Mn_{0.1}O_2$	2.8459(5)	14.158(7)	<0.5
$LiNi_{0.2}Co_{0.6}Mn_{0.2}O_2$	2.8417(1)	14.180(2)	

Table 2
Activation energy of electrical conductivity for $LiNi_{1-y-z}Co_yMn_zO_2$ oxides.

Sample	E_A/eV
$LiNi_{0.75}Co_{0.25}O_2$	0.16
$LiNi_{0.65}Co_{0.25}Mn_{0.1}O_2$	0.18
$LiNi_{0.55}Co_{0.35}Mn_{0.1}O_2$	0.19
$LiNi_{0.4}Co_{0.5}Mn_{0.1}O_2$	0.19
$LiNi_{0.2}Co_{0.6}Mn_{0.2}O_2$	0.30

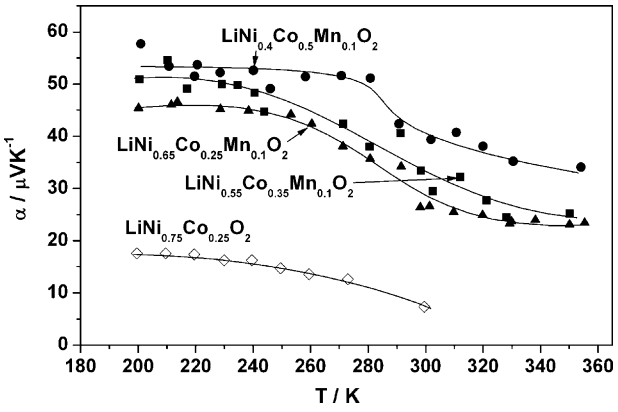

Fig. 3. Temperature dependence of thermoelectric power for $LiNi_{1-y-z}Co_yMn_zO_2$ and $LiNi_{0.75}Co_{0.25}O_2$ oxides.

of the electrical conductivity of this material (Figs. 2 and 3, Table 2). Among $LiNi_{1-y-z}Co_yMn_zO_2$ complex oxides, $LiNi_{0.65}Co_{0.25}Mn_{0.1}O_2$ oxide shows the lowest value of the thermoelectric power what corresponds to the highest effective carriers concentration. This was a reason for which this material was chosen for the studies of transport properties after partial electrochemical deintercalation of lithium in the $Li/Li^+/Li_xNi_{0.65}Co_{0.25}Mn_{0.1}O_2$ cell.

3.3. Structural characterization of deintercalated $Li_xNi_{0.65}Co_{0.25}Mn_{0.1}O_2$ oxide

Cell parameters *a* and *c* versus Li content in deintercalated $Li_xNi_{0.65}Co_{0.25}Mn_{0.1}O_2$ oxide are presented in Fig. 4. In pristine $LiNi_{0.65}Co_{0.25}Mn_{0.1}O_2$ compound Li ions occupying 3a sites screen the electrostatic repulsion between $((Ni,Co,Mn)O_2)_n$ sheets. Extraction of lithium in the range $1 \geq x_{Li} \geq 0.6$ increases repulsion forces between $((Ni,Co,Mn)O_2)_n$ sheets causing increase of *c* parameter (Fig. 4). The observed decrease of *a* parameter in this x_{Li} region is related to the increase of the oxidation state of Ni: $Ni^{2+} \rightarrow Ni^{3+} \rightarrow Ni^{4+}$ and Co: $Co^{3+} \rightarrow Co^{4+}$ transition metal ions. For higher deintercalation degree, $x_{Li} < 0.6$, *c* parameter begins to decrease and *a* parameter starts to increase. It should be noticed that no phase transformation was detected in the analyzed lithium concentration range ($0.3 \leq x_{Li} \leq 1$) in $Li_xNi_{0.65}Co_{0.25}Mn_{0.1}O_2$ oxide. The changes in trends of *a* and *c* parameters with decreasing lithium content in layered $LiNi_{1-y-z}Co_yMn_zO_2$ materials were reported by several authors [11–13]. Some of them suggest that significant overlapping of t_{2g} Co band with the top of the 2p oxygen band can cause that deeper lithium extraction may result in a removal of

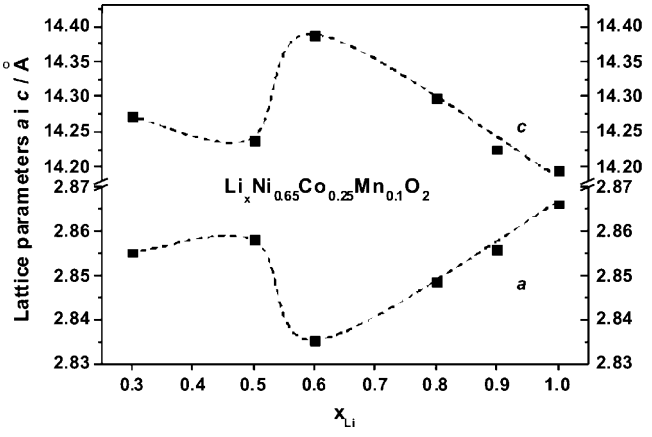

Fig. 4. Change of structural parameters for $Li_xNi_{0.65}Co_{0.25}Mn_{0.1}O_2$ versus Li content.

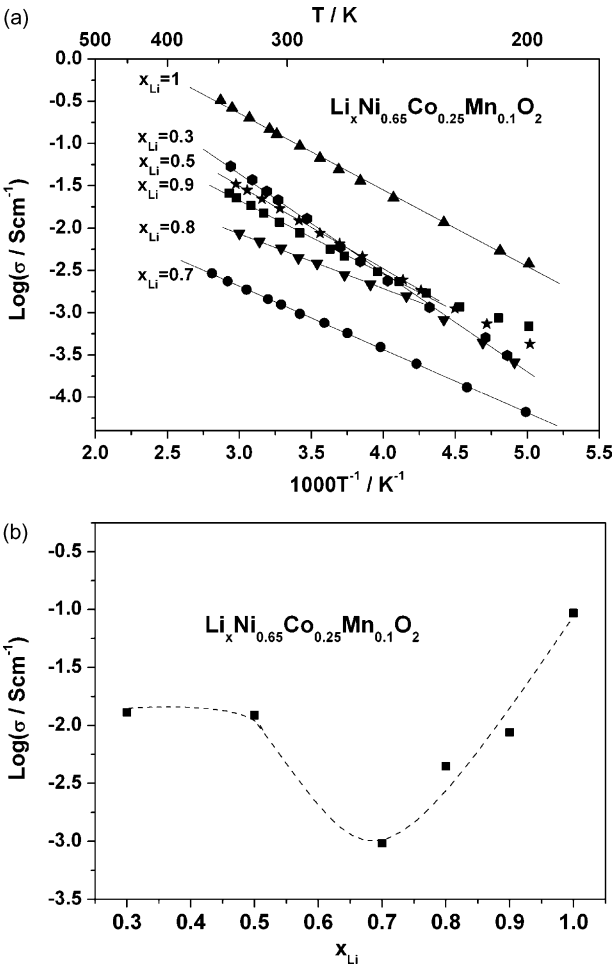

Fig. 5. Electrical conductivity of partially deintercalated $Li_xNi_{0.65}Co_{0.25}Mn_{0.1}O_2$ oxide (a) temperature dependence (b) at room temperature versus Li content.

electrons from the 2p oxygen band. This can lead to the oxidation of oxygen ions and a loss of oxygen from the lattice [12,14]. Following this hypothesis, for $x_{Li} < 0.6$, *c* parameter begins to decrease and *a* parameter starts to increase due to loss of oxygen from the lattice and due to decrease in the oxidation state of transition metals $Co^{4+} \rightarrow Co^{3+}$ and $Ni^{4+} \rightarrow Ni^{3+}$. It might be possible that during deeper lithium extraction two opposite processes run concurrently. It is extraction of lithium and loss of oxygen from the lattice. The second process can be dominant. Limited chemical stability of the considered type of oxides is decisive for the limited reversible cell capacity. To confirm the hypothesis of chemical instability of $Li_{0.5}Ni_{0.65}Co_{0.25}Mn_{0.1}O_2$ oxide further studies of deintercalated samples are needed.

3.4. Electrical properties of deintercalated $Li_xNi_{0.65}Co_{0.25}Mn_{0.1}O_2$ oxide

The temperature dependences of electrical conductivity and thermoelectric power for electrochemically deintercalated $Li_xNi_{0.65}Co_{0.25}Mn_{0.1}O_2$ oxide are presented in Figs. 5a and 6a. A non-monotonous modification of the electrical properties of deintercalated $Li_xNi_{0.65}Co_{0.25}Mn_{0.1}O_2$ oxide is observed. The activation energy of the electrical conductivity for different lithium amount in $Li_xNi_{0.65}Co_{0.25}Mn_{0.1}O_2$ is presented in Table 3.

Better illustration of the modification of electrical properties of $Li_xNi_{0.65}Co_{0.25}Mn_{0.1}O_2$ during deintercalation of lithium is shown in Fig. 5b, which presents electrical conductivity at

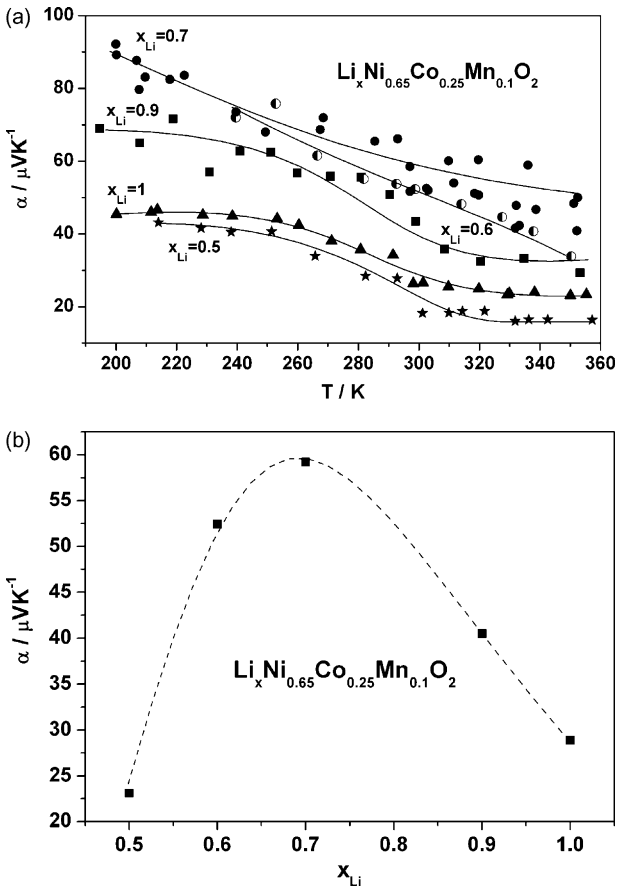

Fig. 6. The thermoelectric power of partially deintercalated $Li_xNi_{0.65}Co_{0.25}Mn_{0.1}O_2$ oxide (a) temperature dependence (b) at room temperature versus Li content.

room temperature versus lithium content. During electrochemical deintercalation of lithium in $0.7 \leq x_{Li} \leq 1$ range deterioration of electrical properties was observed, then for lower lithium content an improvement of electrical conductivity was observed. This behavior is a rare phenomena in deintercalated transition metal compounds. The observed minimum of the electrical conductivity for lithium content $x_{Li} = 0.7$ corresponds well with the maximum of the thermoelectric power values for this composition (compare Figs. 5b and 6b).

In the $LiNi_{1-y-z}Co_yMn_zO_2$ structure, nickel, cobalt and manganese ions have valence $2^+/3^+$, 3^+ and 4^+, respectively. For $LiNi_{0.65}Co_{0.25}Mn_{0.1}O_2$ composition the formula can be formally written as $LiNi^{3+}{}_{0.55}Ni^{2+}{}_{0.1}Co^{3+}{}_{0.25}Mn^{4+}{}_{0.1}O_2$. The electron configuration for $Ni^{2+/3+}$ is $t_{2g}^6e_g^2/t_{2g}^6e_g^1$ and for $Co^{3+/4+}$ is $t_{2g}^6e_g^0/t_{2g}^5e_g^0$. Manganese ($Mn^{4+}$, $t_{2g}^3e_g^0$) is assumed to be electrochemically inactive. Fig. 7 presents a qualitative model of the electronic structure of the starting $LiNi_{0.65}Co_{0.25}Mn_{0.1}O_2$ and deintercalated $Li_{0.5}Ni_{0.65}Co_{0.25}Mn_{0.1}O_2$ oxides, which explains a non-typical modification of the electrical properties of the considered cathode material. As expected, in the deintercalation degree, $x_{Li} > 0.6$, (Figs. 5a, b and 6a, b) the drop of electrical conductivity is related to the extraction of electrons from the e_g Ni band during charge process ($Ni^{2+} \rightarrow Ni^{3+} \rightarrow Ni^{4+}$). For higher deintercalation degree, $x_{Li} < 0.6$, the conductivity increases due to the oxidation of Co^{3+} to Co^{4+} and location of the Fermi level inside a broader t_{2g} Co band. There is also a parallel phenomena (see Section 3.3.) which leads to an improvement of the electrical properties in this x_{Li} region, i.e. the loss of oxygen from the lattice—oxygen leaves the lattice and leaves two electrons, in consequence the concentration of charge carriers increases (electrical conductivity increases).

Table 3
Activation energy of electrical conductivity for different Li content in $Li_xNi_{0.65}Co_{0.25}Mn_{0.1}O_2$.

Sample	E_A/eV
$Li_1Ni_{0.65}Co_{0.25}Mn_{0.1}O_2$	0.18
$Li_{0.9}Ni_{0.65}Co_{0.25}Mn_{0.1}O_2$	0.17
$Li_{0.8}Ni_{0.65}Co_{0.25}Mn_{0.1}O_2$	0.13
$Li_{0.7}Ni_{0.65}Co_{0.25}Mn_{0.1}O_2$	0.15
$Li_{0.5}Ni_{0.65}Co_{0.25}Mn_{0.1}O_2$	0.19
$Li_{0.3}Ni_{0.65}Co_{0.25}Mn_{0.1}O_2$	0.23

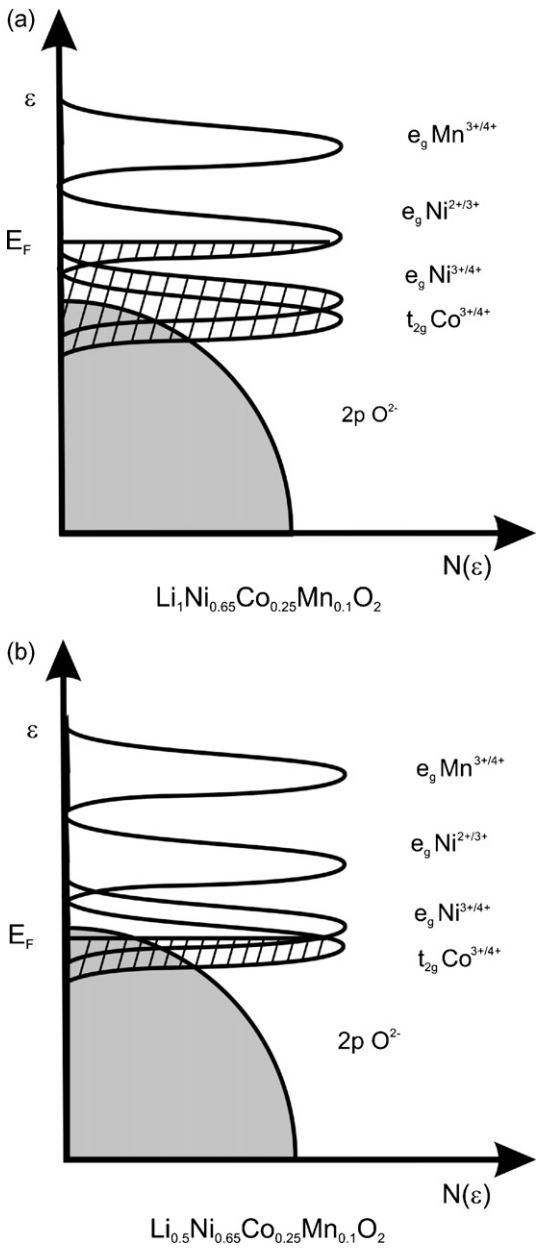

Fig. 7. Simplified qualitative band diagram (a) for starting $LiNi_{0.65}Co_{0.25}Mn_{0.1}O_2$ and (b) deintercalated $Li_{0.5}Ni_{0.65}Co_{0.25}Mn_{0.1}O_2$ oxides.

This type of modification of the electronic properties described for deintercalated $Li_xNi_{0.65}Co_{0.25}Mn_{0.1}O_2$ oxide is distinct from the one observed for $Li_xNi_{0.75}Co_{0.25}O_2$ reference oxide. Electrochemical deintercalation of lithium from $Li_xNi_{0.75}Co_{0.25}O_2$ changes its electrical properties towards metallic ones (Figs. 8 and 9 [6]), what is

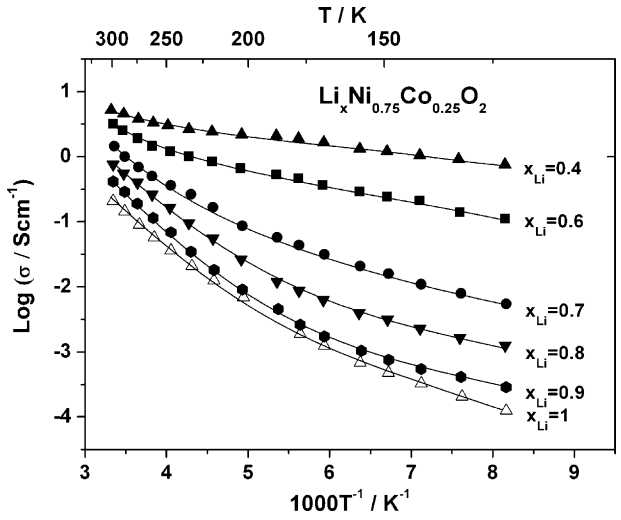

Fig. 8. Temperature dependence of electrical conductivity for deintercalated $Li_xNi_{0.75}Co_{0.25}O_2$ oxide [6].

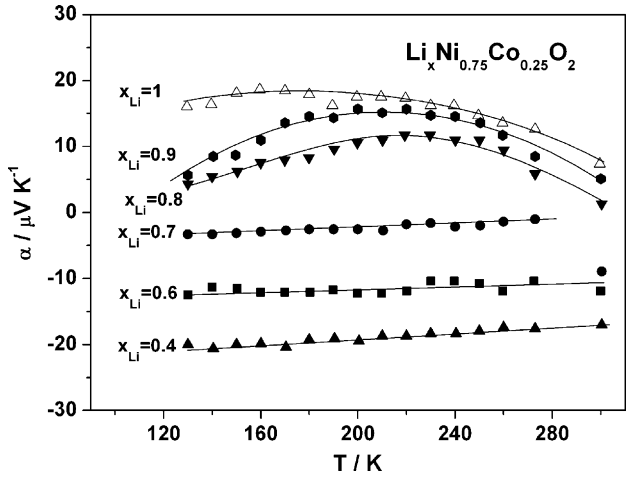

Fig. 9. The temperature dependence of the thermoelectric power for deintercalated $Li_xNi_{0.75}Co_{0.25}O_2$ oxide [6].

related to the decreasing of *a* parameter, i.e. M–M distance, responsible for overlapping of wave functions of d electrons.

4. Conclusion

$LiNi_{1-y-z}Co_yMn_zO_2$ ($y = 0.25$, 0.35, 0.5 and $z = 0.1$) materials were synthesized successfully using soft chemistry EDTA-based method. Investigated oxide cathode materials present good transport properties, with the highest electrical conductivity for $LiNi_{0.65}Co_{0.25}Mn_{0.1}O_2$ oxide. Modification of the structural and the electrical properties during lithium deintercalation exhibits a non-monotonic character. It seems that in the considered group of oxides, $LiNi_{1-y-z}Co_yMn_zO_2$, there is no clear correlation between electrical conductivity and the *a* parameter (M–M distance in the octahedra layers), which is observed for simple, layered transition metal oxides. The increase of *a* parameter and decrease of *c* parameter for $x_{Li} < 0.6$ indicates chemical instability of $Li_xNi_{0.65}Co_{0.25}Mn_{0.1}O_2$ material for lower lithium contents. The further investigations for the optimal chemical composition of the cathode material in $LiNi_{1-y-z}Co_yMn_zO_2$ system are needed in order to improve their chemical stability.

Acknowledgements

The work was supported by the Ministry of Science and Higher Education Republic of Poland under Singapore-Poland Joint Research Project nr SINGAPUR/99/2007.

References

[1] T. Ohzuku, in: G. Pistoia (Ed.), Lithium Batteries, New Materials Development and Properties, Elsevier, 1994.
[2] M. Gozu, K. Świerczek, J. Molenda, J. Power Sources 194 (2009) 38–44.
[3] A.C. Larson, R.B. Von Dreele, Los Alamos Natl. Lab. Rep. LAUR (2004) 86–748.
[4] B.H. Toby, J. Appl. Cryst. 34 (2001) 210–221.
[5] P. Wilk, J. Marzec, J. Molenda, Solid State Ionics 157 (2003) 109–114.
[6] P. Wilk, J. Marzec, J. Molenda, Solid State Ionics 157 (2003) 115–123.
[7] W. Li, J.N. Reimers, J.R. Dahn, Solid State Ionics 67 (1993) 123–130.
[8] J. Choi, A. Manthiram, Solid State Ionics 176 (2005) 2251–2256.
[9] J. Molenda, A. Stokłosa, T. Bąk, Solid State Ionics 36 (1989) 53–58.
[10] J. Molenda, P. Wilk, J. Marzec, Solid State Ionics 146 (2002) 73–79.
[11] J.-M. Kim, N. Kumagai, S. Komaba, Electrochim. Acta 52 (2006) 1483–1490.
[12] J. Choi, A. Manthiram, J. Electrochem. Soc. 152 (2005) A1714–A1718.
[13] L.A. Montoro, J.M. Rosolen, Electrochim. Acta 49 (2004) 3243–3249.
[14] A. Manthiram, J. Choi, J. Power Sources 159 (2006) 249–253.